Antifreeze peptides from Litopenaeus vannamei head

The cryoprotective effect of *Litopenaeus vannamei head-derived* peptides and its ice-binding mechanism

Julieth Joram Majura [a], Xiujuan Chen [a], Zhongqin Chen [a,b,c], Mingtang Tan [a,b,c], Guoping Zhu [a,b,c], Jialong Gao [a,b,c], Haisheng Lin [a,b,c], Wenhong Cao [a,b,c,*]

[a] *College of Food Science and Technology, Guangdong Ocean University, Zhanjiang 524088, China*
[b] *Guangdong Provincial Key Laboratory of Aquatic Products Processing and Safety, Guangdong Provincial Engineering Technology Research Center of Seafood, Zhanjiang 524088, China*
[c] *Guangdong Province Engineering Laboratory for Marine Biological Products, Zhanjiang 524088, China*

ARTICLE INFO

ABSTRACT

Although discarded as waste, shrimp heads are a potential source of antifreeze peptides, which can be used as cryoprotectants in the food industry. Their utilization in frozen foods can help mitigate the negative effects caused by the freezing technique. *Litopenaeus vannamei* shrimp heads were autolyzed, and the shrimp head autolysate (SHA) was separated *via* ultra-filtration and ion exchange chromatography. The antifreeze effect of SHA on the biochemical properties of myofibrillar proteins of peeled shrimps during five freeze-thaw cycles was evaluated. Peptide screening was done using the LC-MS/MS technique. A molecular docking (MD) study of the interaction between ice and shrimp head-derived antifreeze peptides was done. Results showed that shrimp-head autolysate has a maximum thermal hysteresis value of 1.84 °C. During the freeze-thaw cycles, the shrimp-head autolysate exhibited an antifreeze effect on frozen peeled shrimps. 1.0 and 3.0%-SHA groups showed significantly lower freeze denaturation than the negative control group. The muscle tissues of SHA-treated groups were not as severely damaged as the negative control group. The molecular docking study revealed that the shrimp head-AFPs bound to ice *via* hydrogen bonding, and both hydrophilic and hydrophobic amino acid residues were involved in the ice-binding interactions. 6 ice-binding sites were involved in the peptide-ice interaction. Our findings suggest that shrimp head-derived AFPs can be developed into functional additives in frozen foods and add more insights into the existing literature on antifreeze peptides.

1. Introduction

Freezing is extensively used as a means of food storage for longer periods. Some advantages associated with freezing foods include low cost, long-term storage, convenience, and retarded microbial growth (Sun et al., 2023). Despite the advantages, freezing has also been associated with detrimental effects such as moisture/drip loss, membrane rapture, disorientation of the cellular structure in muscular foods, protein denaturation, and lipid oxidation, lowering its quality (Dawson et al., 2018; Lee et al., 2016; Lorentzen et al., 2020).

Ice formation and growth is a substantial hurdle with significant technological consequences (Olijve et al., 2016). During frozen storage, water in the surrounding environment or the food matrix freezes and expands, affecting the structural integrity of muscles (Zhang et al., 2022). Enormous efforts have been expended in designing and applying cryoprotectants within food systems to surmount this obstacle, thereby guaranteeing the preservation of nutritional and sensory attributes in frozen foodstuffs. Antifreeze proteins/peptides, salts, saccharides, glycerol, and natural deep eutectic solvents (NADES) have been used as antifreeze materials (Sun et al., 2023). Unlike other antifreeze materials, AFPs are considered safe and better cryoprotectants since they exhibit a thermal hysteresis effect, a unique ability to lower the freezing point of water in a non-colligative manner; hence, this attracts their use to preserve frozen food (Baskaran et al., 2021; Krichen et al., 2018).

Shrimp is considered a high-value seafood due to its nutrient abundance, easy cultivation, delicacy, and texture. Shrimp head, along with its viscera, shells, and tail, is a common byproduct in shrimp processing plants. Protein present in shrimp heads can be recovered and utilized as an alternative protein source, for instance in fish and animal feed (Abuzar et al., 2023). Antifreeze peptides for use as cryoprotectants in

food can also be extracted from this inexpensive protein source. Our previous study confirmed that *Litopenaeus vannamei* shrimp head autolysate has thermal hysteresis activity (Majura et al., 2023).

The advancement of research in AFPs and their applications are often hindered by factors such as high production costs, limited availability, and structural complexity of the peptides (Gandini et al., 2020). Commercial proteases are extensively used to extract bioactive components despite their high costs. However, the economic implications of these enzymes cannot be overlooked (Cahú et al., 2012), especially if it is a massive production of protein hydrolysates from the by-products (Nikoo et al., 2021). In contrast, the autolytic recovery of proteins from shrimp heads presents a more cost-effective alternative. This process relies on the inherent proteases in shrimp for protein hydrolysis, thereby reducing the overall cost. Furthermore, advancements in biotechnology have largely contributed to the progress of bioactive peptides. For instance, molecular docking and simulation studies have enhanced our understanding of the interaction between antifreeze proteins/peptides and ice (Jiang et al., 2022).

Recently, studies have been carried out to explore antifreeze peptides from protein hydrolysates of various marine byproducts (Cao et al., 2023; Dang et al., 2022; Nikoo et al., 2019). In their study on antifreeze peptides, Zhu and team confirmed that the autolysate from Southern rough shrimp byproducts has a thermal hysteresis effect and the ability to reduce freeze denaturation. To the best of our knowledge, there is no research work so far that has explored the antifreeze effect of peptides derived from Pacific white shrimp heads. This present study highlights the antifreeze effect of shrimp head autolysate and investigates the ice-binding mechanism of shrimp head-derived antifreeze peptides. We utilized peeled Pacific white shrimps as the experimental objects to assess the antifreeze effect of the shrimp head autolysate during five freeze-thaw cycles. Molecular docking techniques were employed to elucidate the binding mechanism of the identified antifreeze peptides on ice.

2. Materials and methods

2.1. Chemical reagents

The total sulfhydryl kit was purchased from Beijing Boxbio Science & Technology Co., Ltd (Beijing, China), the Ca^{2+}-ATPase activity kit from Jianjian Bioengineering Institute (Nanjing, China), Bromophenol (BPB) was purchased from Shanghai Yien Chemical Technology Co., Ltd (Shanghai, China). Biuret protein assay kit from Beijing Leagene biotech. Co., ltd (Beijing, China), Maleic acid from Shanghai Macklin Biochemical Technology Co., Ltd (Shanghai, China), Capto-Q from Beijing Zhongyuan Heju Biotechnology Co., Ltd (Beijing, China). All reagents were of analytical grade.

2.2. Autolysis and separation of shrimp head autolysate

In our previous study, 5 h autolysis time yielded shrimp head autolysate with a higher thermal hysteresis activity, measured at 1.82 °C (Majura et al., 2023). Briefly, the shrimp heads were blended with distilled water at a substrate/water ratio of 23% w/v. The mixture was homogenized for 1 min, and the pH of the homogenate was adjusted to 7.0 using 1 M HCL and 1 M NaOH. The homogenate was then placed in a water bath (temperature: 50 °C) for 5 h for autolysis to take place. After 5 h, the autolysate was heated at 90 °C for 10 min to terminate the autolytic process, and the autolysate was then centrifuged for 10 min (rotation speed: 9000 rpm, temperature: 4 °C). After centrifugation, the supernatant was collected and sequentially passed through an ultrafiltration membrane using a 3000 Da molecular weight cutoff in an Amicon-stirred ultrafiltration cell. The <3000 Da permeate was collected, concentrated, and freeze-dried.

Further separation of the <3000 Da permeate using ion exchange chromatography was carried out. 10 mg/mL of the collected permeate

was filtered through a 0.22 μm membrane to eliminate impurities. Ultrapure water was added to the bottom of the chromatographic column to remove air at the lower part of the column. The Capto-Q was slowly added, and the column was pressed with ultrapure water at a 10 mL/min flow rate. After pressing the column, the flow rate was adjusted to 8 mL/min, and the column was equilibrated with 50 mmol/L Tris-HCl (pH = 8.0) buffer. Once the column was stable, the sample solution was added. The sample concentration was 10.0 mg/mL, and the sample volume was 8 mL. 50 mmol/L Tris-HCl (pH = 8.0) buffer was used as elution A and 1.0 mol/L NaCl as elution B. The flow rate was set at 6 mL/min, and 8 mL was collected in each tube. The elution program was set as follows: 100% A liquid isocratic elution; 100% A liquid-50% A liquid linear elution; 100% B liquid isocratic elution. The absorbance of the elution curve was measured at 220 nm, and each peak was collected. The collected fractions were desalted by dialysis, concentrated, and freeze-dried.

2.3. Determination of the thermal hysteresis activity

The TH activity of the permeate was measured using a differential scanning calorimeter (DSC) according to our previous study (Majura et al., 2023). 10.0 μL of the shrimp head autolysate (10 mg/mL) was put into the sample cell and cooled to −25 °C at a rate of 5 °C/min. The sample was held at this temperature (−25 °C) for 2 min, then heated to 25 °C at the same rate of 5 °C/min. The melting enthalpy (ΔH_m) was determined from the DSC curve. The sample was then heated up to 25 °C at the speed of 5 °C/min and cooled to −25 °C at the speed of 5 °C/min. The sample was kept at −25 °C for 2 min. The melting temperature (T_m) and enthalpy of melting (ΔH_m) of shrimp-head autolysate were calculated from the DSC curve. The sample was then cooled down from 25 °C to −25 °C at 5 °C/min for 2 min. After rising to −5 °C at the rate of 5 °C/min, the sample was then heated to the holding temperature (T_h) at a rate of 5 °C/min. The sample was held at T_h for 2 min, then cooled to 25 °C at the rate of 5 °C/min and held at a different T_h for 2 min. The TH activity of the sample was calculated using equation (1).

$$TH = T_h - T_0 \tag{1}$$

2.4. Sample preparation and extraction

2.4.1. Sample preparation

Fresh *Litopenaeus vannamei* shrimps with an estimated 12–15 mm length were bought from Huguang Aquatic Market, Zhanjiang. The shrimps were placed in a cooler box (temperature: 4 °C) and quickly transported to the laboratory. The shrimps were then beheaded, and the shells were peeled off for abdominal muscle. By random selection, the peeled shrimps were divided into five different groups. 0.5% of the commercial phosphate was added to one group and labeled 0.5% positive control (PC). For the shrimp-head autolysate groups, 0.5, 1.0, and 3.0% of the shrimp-head autolysate were added, and the groups were labeled according to the concentration added. An untreated group was used as a negative control (control). The samples were quickly frozen at −80 ± 2.0 °C for 72 h.

2.4.2. Extraction of myofibrillar protein

Following a 72-h freezing period, the shrimp samples were transferred to a refrigerator set at 4 °C and allowed to thaw entirely for 1 h. 2.0 g of shrimp sample (fresh/thawed) was treated with 20 mL Tris-Maleate buffer (20 mM, pH 7, with 0.05 M KCl), homogenized for 1 min, and centrifuged for 15 min (rotation speed: 10,000 rpm at 4 °C). After centrifugation, the supernatant was discarded, and 20 mL of the tris-maleate was added, homogenized, and placed at 4 °C for 30 min to allow further extraction of the proteins. Afterward, the sample was centrifuged at the same conditions, and the supernatant was again
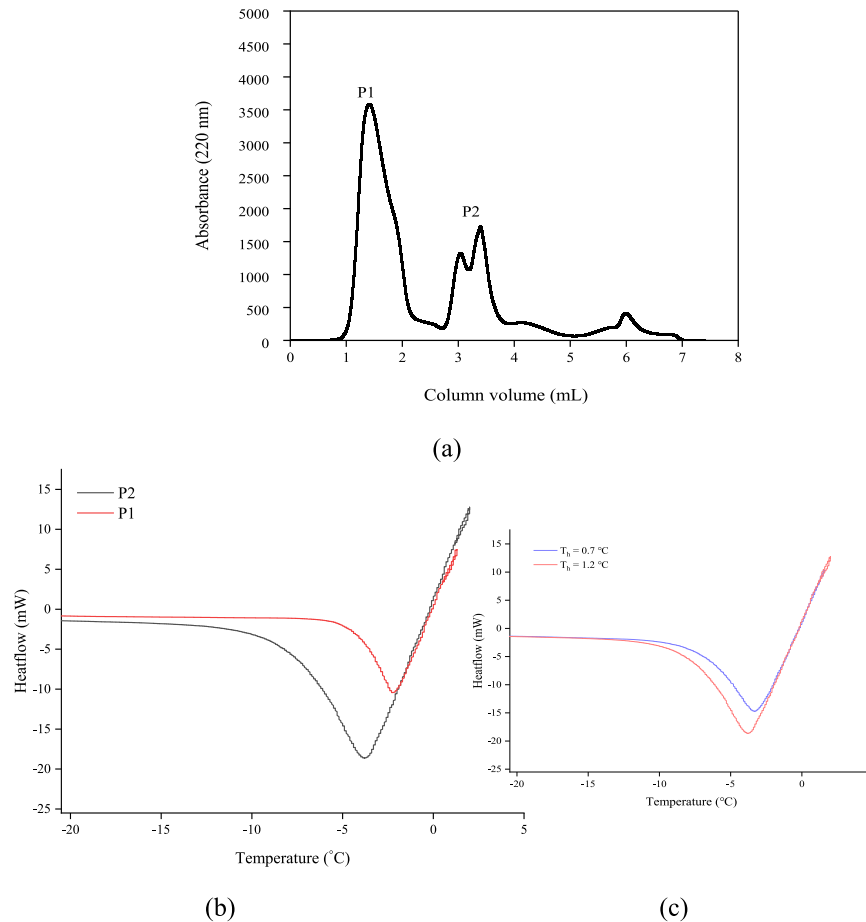
Fig. 1. Ion-exchange chromatography elution profile of shrimp head autolysate (a). The DSC thermogram of collected fractions is denoted by P1 and P2 (b). DSC thermogram of P2 at two T_h (c). P1 and P2 denote fractions with little TH activity and higher TH activity, respectively.

discarded. 20 mL of the same buffer was added and homogenized, and the homogenate sample was centrifuged for 10 min (rotation speed: 6000 rpm, temperature: 4 °C). Finally, the supernatant was collected and immediately used to evaluate the antifreeze effect.

2.5. Evaluation of antifreeze effect on myofibrillar proteins

The antifreeze effect of the shrimp head autolysate on the myofibrillar proteins was done by measuring the biochemical changes: soluble protein content, Ca^{2+}-ATPase activity, total sulfhydryl content, and surface hydrophobicity of myofibrillar proteins after freeze-thawing cycles. Structural changes in the muscle tissues were also observed after hematoxylin-eosin staining.

2.5.1. Determination of salt soluble myofibrillar protein content
MP content of each sample group was determined using a biuret protein assay kit. 20 μL of the myofibrillar-containing supernatant was added to a microwell plate, and 200 μL of the working reagent was added next. The microwell plate was shaken and incubated for 15 min. The absorbance of each sample was then measured at 540 nm.

Triplicates were made for each sample group. The protein concentration for each sample group was calculated from the equation: $y = 0.0116x + 0.0918$.

2.5.2. Total sulfhydryl content
The total sulfhydryl content in each sample group was determined using a sulfhydryl kit, following the manufacturer's instructions precisely. Two parallel groups were made for each sample: test and control. For the test group, 40 μL of extracted MP was transferred to a tube. Then, 150 μL of reagent 1 and 10 μL of reagent 2 were added. For the control group, 10 μL distilled water was added instead of reagent 2. The sample was mixed thoroughly and incubated at room temperature (25 ± 1.0 °C) for 10 min, and the absorbance was measured at 412 nm. The total sulfhydryl content for each sample group was calculated from the equation: $y = 2.8303x + 0.5273$.

2.5.3. Surface hydrophobicity
The surface hydrophobicity of each sample group was determined as described by (Chen et al., 2022) with some modifications. 5.0 mL of the myofibrillar-containing supernatant was transferred to a centrifuge tube

with 1.0 mL bromophenol (1.0 mg/mL) and thoroughly mixed for 1 min. The mixture was then incubated at room temperature (25 $\pm$ 1.0 °C) for 7 min before centrifugation at 7000 rpm for 15 min. After centrifugation, 0.1 mL of the supernatant was added to a tube containing 0.9 mL distilled water, mixed thoroughly, and the absorbance of each sample group was measured at 595 nm. 1.0 mL of 20 mM phosphate buffer solution (PBS) in 0.2 mL of 1.0 mg/mL bromophenol was used as a blank solution. The surface hydrophobicity of MP was determined by the amount of MP bound to bromophenol using equation (2) below.

$$\text{Surface hydrophobicity } (\mu g \, / \, mL \,) = \frac{A_0 - A_1}{A_0} \times 200 \tag{2}$$

Where A_0 is the absorbance value of the blank at 595 nm, A_1 is the absorbance value of the sample at 595 nm.

2.5.4. Microstructure observation

The preparation and observation of the microstructure of the peeled shrimps were done according to a previous method (Shi et al., 2022) with slight modifications. Thawed peeled shrimp was cut into long strips (1.0 × 1.0 × 1.0 cm^3) and immediately placed in a 4.0% formaldehyde solution for fixation for 24 h. The samples were then washed thrice with deionized water and dehydrated using ethanol solutions of different concentrations (50, 70, 80, 90, and 100%). The specimens were embedded in paraffin, sectioned (4.0 μm), dried, deparaffinized, and stained with hematoxylin-eosin (H&E) staining solution, and the structure of the muscle tissues was observed under a light microscope (Nikon).

2.6. Screening of antifreeze peptides

Liquid chromatography-tandem mass spectrometry was employed for peptide screening according to the parameters provided by the manufacturer. Liquid A was 0.1% formic acid aqueous solution, and liquid B was 0.1% formic acid acetonitrile aqueous solution (acetonitrile was 84%); the liquid chromatography column (0.15 mm × 150 mm, RP-C18, Column Technology Inc.) was equilibrated with 95% of the Liquid A. The samples were uploaded into an autosampler to Zorbax 300SB-C18 peptide traps (Agilent Technologies, Wilmington, DE) and separated by capillary high-performance liquid chromatography-mass spectrometry analysis was performed on a Q Exactive mass spectrometer with positive ion detection for 65 min. For peptide sequence analysis, the typical peaks from the mass spectrometry test were searched for in the corresponding databases using the software MaxQuant (MUC, Germany). Parameters were set as follows: the protein modifications were carbamidomethylation (C) (fixed), oxidation (M) (variable), Acetyl (Protein N-term) (variable); the enzyme specificity was set to Unspecific; the maximum missed cleavages were set to 2; the precursor ion mass tolerance was set to 20 ppm, and MS/MS tolerance was 20 ppm. UnitProt database was used as a reference to confirm the identified peptides.

2.6.1. Characterization and molecular docking of identified AFPs

Prediction of antifreeze peptides was performed using the Cryo-Protect. web server (https://codes.bio/cryoprotect), accessed on April 2024. The molecular weight, isoelectric point, and instability index of the antifreeze peptides were analyzed using the online ProtParam tool (https://web.expasy.org/protparam/), accessed on April 2024. The secondary structure of each AFP was analyzed by the Phd prediction server (Combet et al., 2000).

2.7. Ice-binding mechanism of AFPs

Molecular docking was done to study the interaction of the selected antifreeze peptides with ice. Before docking, the peptides were drawn using the ChemDraw software, and their three-dimensional structures were obtained on Chem3D software after their energy was minimized using the MM2 forcefield. Molecular docking was performed using the Autodock Vina software to understand the interaction of the peptides with the ice/water surface. Ice was selected as the receptor, and peptide as the ligand. The docked peptide-ice/water complexes were visualized on the Discovery Studio software, and the nature of binding, binding type, distance, and binding sites were obtained.

2.8. Statistical analysis

Triplicates were done for each sample group, and a minimum of three parallel experiments were carried out to eliminate random errors. Data are expressed as mean $\pm$ standard deviation (SD) and were subjected to one-way ANOVA with Duncan's multiple range test using SPSS 20.0 (IBM Corp., Armonk NY, USA). $P < 0.05$ shows that the data are significantly different. Figures were plotted using Origin Pro 2021 (Origin Lab Corp., MA, USA).

3. Results and discussion

3.1. TH determination of separated fractions

Thermal hysteresis is a valuable indicator of the antifreeze activity of a substance (Ortiz et al., 2021). After ultrafiltration and ion exchange chromatography, the TH of each peak was determined. The presence of more than a single peak during ion chromatography indicates that the components of a sample were separated based on their ionic charge and affinity for the ion exchange (Harcum, 2008). As shown in the ion-chromatogram in Fig. 1(a), two peaks were obtained from the column. Fig. 1(b) shows the thermograms of peaks 1 and 2. The measured thermal hysteresis activity of P1 and P2 was 0.05 °C and 1.84 °C, respectively. The smaller TH value for P1, 0.05 °C, indicates that the fraction likely contained very little to no antifreeze peptides. P2 showed a delay of the crystallization peak at two different holding temperatures, which was slightly further delayed when the holding temperature was 1.2 °C, as depicted in Fig. 1(b). From this TH value alone, we observe that the shrimp head autolysate has antifreeze properties and can help prevent ice crystal growth in food during freezing.

Before separation, the shrimp head autolysate had a TH value of 1.82 °C; the ultrafiltration and ion exchange chromatography techniques show to have caused an increase of its value by 0.02 °C. A study on antifreeze peptides from *Takifugu obscurus* skin by Yang et al. showed increased TH after the separation and ion exchange chromatography processes (Yang et al., 2022). The TH value of 1.84 °C of the shrimp head autolysate is slightly higher than the TH value of 1.57 °C of synthetic AFPs from Southern rough shrimp (Zhu et al., 2022).

3.2. The antifreeze effect of shrimp head autolysate on peeled shrimps during F-T cycles

Myofibrillar protein is a vital component of seafood muscle tissue. The quality of myofibrillar proteins is considered the most critical aspect because it affects the protein intermolecular interactions and physical stability (Dara et al., 2021).

3.2.1. Salt-soluble protein content

Fresh shrimp had a myofibrillar protein content of 3.29 mg/g, which decreased with increasing freeze-thaw cycle. Fig. 2(a) shows the protein content of the sample groups during each F-T cycle. The protein content in the 3.0%-SHA and 0.5% PC sample groups was significantly higher than in the others. Significant changes were observed in all groups in the third freeze-thaw cycle. The control group had the lowest protein content by the end of the five freeze-thaw cycles, 0.45 mg/g. The MP content of the SHA-treated groups: 0.5, 1.0, and 3.0% decreased by 78, 77.8, and 69%, respectively. Overall, the protein content decreased with an increasing number of F-T cycles.

The decreasing protein content resulted from repeated freeze-thaw cycles, which caused the formation of ice crystals, further damaging the muscle fibers and leading to protein degradation. In their study, Wan and team showed that the myofibrillar proteins from mirror carp were degraded following five freeze-thaw cycles, causing a significant decrease in MP solubility (Wan et al., 2023). Freeze denaturation is common in myofibrillar proteins. Proteins can undergo unfolding caused by destabilizing forces, which increase with temperature fluctuation. When the temperature fluctuates during storage, it can deteriorate the quality of the food product (Ramirez-Guerra et al., 2012).

3.2.2. Ca^{2+}-ATPase activity

Ca^{2+}-ATPase activity is a helpful indicator of myofibrillar protein denaturation at low-temperature storage (Walayat et al., 2021). Reduced Ca^{2+}-ATPase activity confirms the occurrence of myosin denaturation (Jommark et al., 2018). Generally, the Ca^{2+}-ATPase activity decreased ($P < 0.05$) during the frozen storage in all sample groups, as shown in Fig. 2(b). A rapid activity loss was observed in all samples on the first F-T cycle. Ca^{2+}-ATPase activity reduced from 0.58 to 0.02, 0.10, 0.02, 0.14 μmol Pi/mg/min and 0.05 μmol Pi/mg/min in control, 0.5%-PC, 0.5, 1.0, and 3.0%-SHA groups, respectively. The control and 0.5%-SHA groups had the lowest Ca^{2+}-ATPase activity by the end of the F-T cycles. However, the residual Ca^{2+}-ATPase activity in the 1.0%-SHA group was higher than all the other sample groups throughout the five freeze-thaw cycles, this suggests that the shrimp-head autolysate to a certain degree delayed the loss of the Ca^{2+}-ATPase activity.

A similar trend of the reduction of Ca^{2+}-ATPase activity with increasing F-T cycles was also observed in previous studies. A decrease in the Ca^{2+}-ATPase activity was also observed in Pacific white shrimp subjected to three freeze-thaw cycles (Jommark et al., 2018). During frozen storage, ice crystals tend to form, causing disruptions in protein network interactions. Such disruptions affect the native protein conformational structure. These structural changes and the rearrangement of the interactions between proteins may cause the loss of Ca^{2+}-ATPase activity (Masson and Lushchekina, 2022).

3.2.3. Total sulfhydryl groups

Sulfhydryl groups are among the most active groups in proteins and substantially impact the functional characteristics of a protein molecule (Wan et al., 2023). Also, the sulfhydryl groups of myofibrillar proteins are more susceptible to oxidation and may be converted to disulfide bonds during freeze-induced changes (Walayat et al., 2021). The effect of the freeze-thaw cycles on the total sulfhydryl groups of the myofibrillar proteins was studied, and the results are shown in Fig. 2(c). The concentration of the total sulfhydryl groups showed a declining trend with increasing F-T cycles. Initially, the total content was 0.39 μmol/g in the fresh group, followed by a significant drop in the sulfhydryl content after the first freeze-thaw cycle in all groups. However, a slow decline of the sulfhydryl groups was observed in the treated groups (1.0 and 3.0%-SHA) compared to that of the untreated group (negative control), this implies that the shrimp-head autolysate as a cryoprotectant played a role in preserving the sulfhydryl groups.

3.2.4. Surface hydrophobicity

The formation of ice during freezing disrupts the native three-dimensional structure of a protein and exposes the buried hydrophobic groups (Walayat et al., 2021). Initially, the fresh shrimps had a surface hydrophobicity value of 169.6 μg. The changes in hydrophobicity values during storage are shown in Fig. 2(d). The increase in hydrophobicity was observed in all the groups, with a rapid increase in the control group. In the SHA-treated groups, it can be observed that there was an inverse proportion between the concentration of the SHA
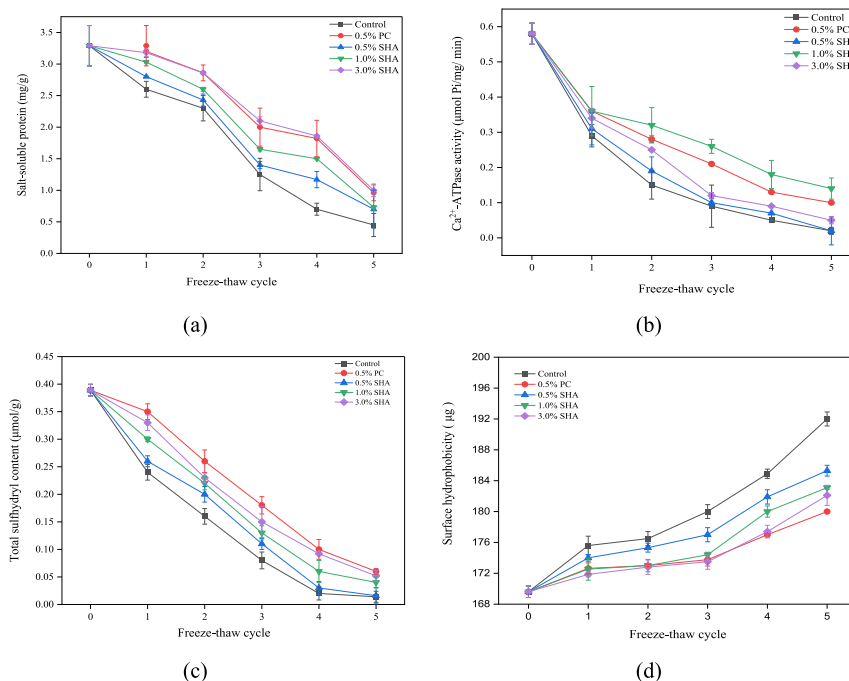

(a)

(b)

(c)

(d)

Fig. 2. shows salt soluble protein content (a), Ca^{2+}-ATPase activity (b), total sulfhydryl content (c), and surface hydrophobicity (d) of peeled shrimps during F-T cycles.
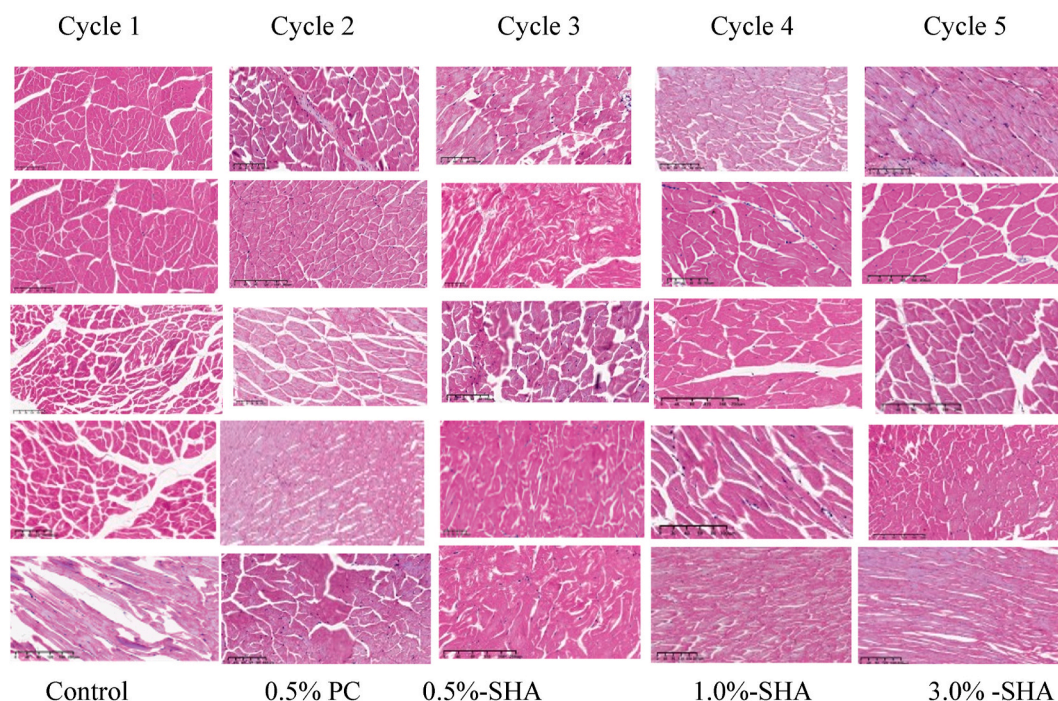
Fig. 3. Microstructure observation of peeled shrimp during F-T cycles.

and surface hydrophobicity; the surface hydrophobicity increased with decreasing SHA concentration. The 0.5%-SHA group had a higher surface hydrophobicity than the 1.0 and 3.0%-SHA treated groups.

Previous studies have confirmed that multiple freeze-thaw cycles may affect the physiochemical properties of a protein, including an increase in its surface hydrophobicity. After nine freeze-thaw cycles, there was a vivid increase in the surface hydrophobicity of soy protein isolate (Wang et al., 2023). From the DSC results, the shrimp head autolysate can exhibit thermal hysteresis activity (1.84 °C), thus lowering the freezing point of water. As a result, this might have delayed the growth of ice crystals and water migration to an extent.

3.2.5. Microstructure observation

Myofibrillar denaturation of muscle myofibers is indicated by clear spaces between and within the myofibers (Yan et al., 2023). All sample groups had obvious extracellular spaces (white gaps) between the myofibrils, as shown in Fig. 3. The myofibrils were ruptured, resulting in fragments in between them. By the fifth freeze-thaw cycle, the control group had extensive white gaps compared to the treated groups. Also, in 1.0 and 3.0%-SHA treated groups, it can be observed that the myofibrils of 1.0 and 3.0%-SHA treated groups appeared firmer than those of the 0.5%-PC group. Both freezing and thawing processes affect the structure of muscle tissues. As stated earlier, freezing causes rapture of the cellular membrane in muscle tissue, affecting its native structure. The thawing process, on the other hand, causes mechanical damage to the muscles, and the resulting water cannot be entirely reabsorbed by the muscle fibers, resulting in moisture loss and a consequent reduction in nutrients. The formation of large ice crystals during the freeze-thaw cycle can compress and damage the microstructure of muscle fibers, expanding the space between these fibers (Du et al., 2021).
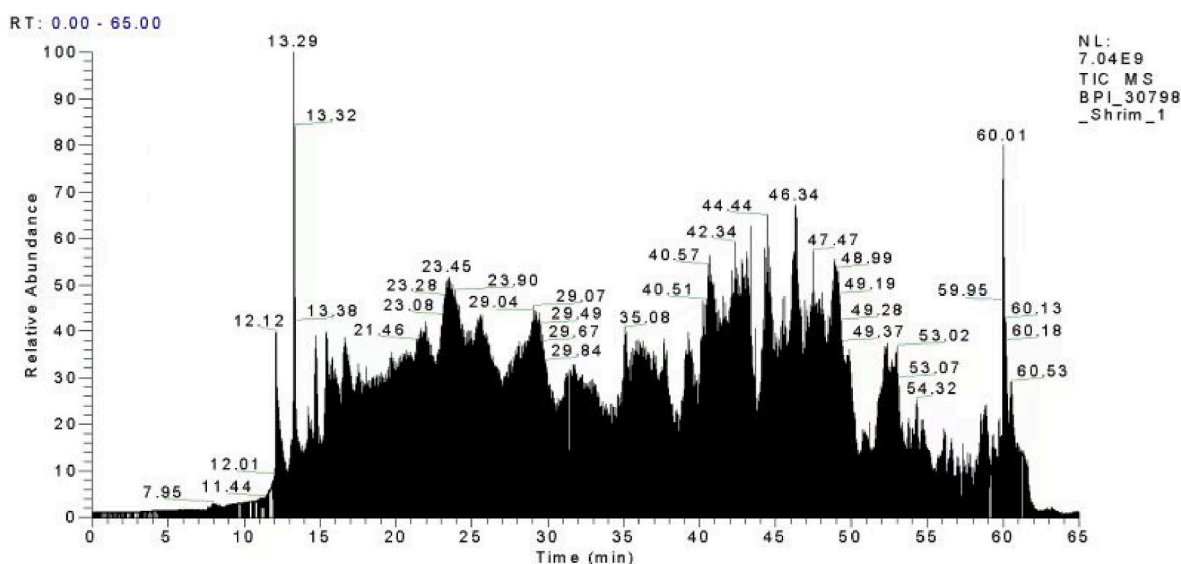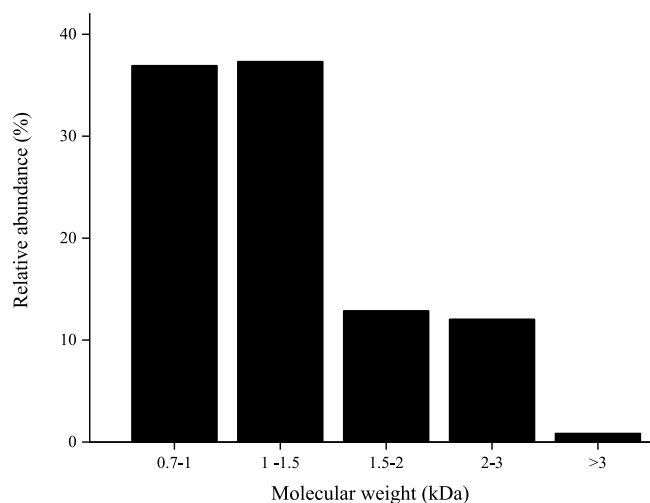

Fig. 4. Total ion chromatogram by LC-MS/MS analysis.

Table 1
Peptide sequences corresponding to typical peaks on the total ion chromatogram.

Peptide	m/z ratio	MW (Da)	Peptide	m/z ratio	MW (Da)
LPPLYEV	60.13	829.46	EHVVLPPLYEVTP	49.37	1491.50
LVQELND	60.53	829.82	LEPIEHAF	47.47	954.48
GGKKPHRYRPGT	53.07	1352.74	LMLFDVLM	12.12	1012.50

Fig. 5. The relative abundance of peptide sequences retrieved during LC-MS/MS analysis.

3.3. Screening, characterization, and identification of AFPs

A total of 239 peptide sequences were retrieved after the completion of the analysis in 65 min, as shown in the total ion chromatogram (Fig. 4). The typical peaks corresponding to specific peptides are shown in Table 1. As shown in Fig. 5, 87.06 % of the peptides had a <2000 Da molecular weight range, while those with molecular weight between 2000 and 3000 and > 3000 Da constituted 12.03 and 0.83%, respectively. Previously, it was shown that SHA had a significantly higher abundance of components with a molecular weight of <500 Da (Majura et al., 2023); unfortunately, these low molecular weight components might have been underrepresented during the LC-MS/MS analysis. Based on amino sequence length, over 70% of the antifreeze peptides had a sequence length between 7 and 15, which is considered an ideal length for AFPs (Pratiwi et al., 2017). Generally, the identified peptides contained both hydrophilic and hydrophobic amino acid residues. It can be observed that glutamic acid, alanine, glycine, isoleucine, methionine, proline, aspartic acid, and threonine residues were prominent in these peptides. This aligns with the results of the amino acid composition of the 5 h-shrimp head autolysate, which showed a higher content of glutamic acid, aspartic acid, and glycine (Majura et al., 2023).

Out of 239 only 123 peptide sequences were classified as AFPs, as presented in Table S1. The identified AFPs were mainly derived from hemocyanin and trypsin. Antifreeze peptides with an instability index greater than 40 were excluded. Only stable peptides with a peptide sequence length between 7 and 15 were selected, hence a total of 23 antifreeze peptides were further selected for molecular docking. The binding energy can provide insights into the compatibility of the receptor-ligand complex after docking. A more negative binding energy indicates a stronger interaction and, thus, a stabler complex (Forli et al., 2016). Based on this factor, only 8 peptide-ice/water complexes: EAAEHLVQEYKDHRL, DGEHGGSHSLCGAH, GELNQDVDEGTEQT, TAGNFEMEFTGT, EGGIGTGNTVYPPLS, GGKKPHRYRPGT, IMNDRGADV and PVQHFALKDMET were further selected for visualization.

3.3.1. Ice-binding mechanism

Antifreeze proteins/peptides bind to the ice surface through hydrogen bonding, hydrophobic interactions, and van der Waals forces (Lee, 2019). In this study, hydrogen bonding was the primary force involved in ice binding, as shown in Fig. 6. From the peptides, hydrogen bonding interactions were formed between the O atom of the hydroxyl group, the carbonyl group, and the N and H atoms of the amine group. Also, it can be observed that each of the peptides had two faces: (i) the ice-binding face (IBF) and (ii) the non-ice-binding face (NIBF).

Pro, Asp, Glu, Gly, Thr, Ser, Met, Leu, Arg, Val, and others were involved in ice-binding, as shown in Table 2. This aligns with the findings of other scholars who confirmed the presence or abundance of these amino residues to the ice-binding property of an antifreeze peptide/protein (Baardsnes et al., 2001; Fu et al., 2019; Graham and Davies, 2005; Yang et al., 2022). EAAEHLVQEYKDHRL and GELNQDVDEGTEQT had the highest number of binding sites (6) compared to the rest of the sequences.

Several factors influence the antifreeze activity of an antifreeze peptide, including amino acid composition, hydrophobicity, isoelectric point, and secondary structure. Studies have argued that the hydrophilic amino acid residues are majorly responsible for interaction with ice, giving the peptide its antifreeze property (Knight et al., 1993; Tyshenko et al., 1997; Zhu et al., 2022). While this is true, hydrophobic amino residues are also involved in ice-binding. Our previous study on the physiochemical properties of shrimp-head autolysate found that the thermal hysteresis activity and hydrophobic amino acid content of the shrimp-head autolysate had a positive correlation (Majura et al., 2023). Hydrophobic amino residues: Phe, Leu, Tyr, Val, and Ile were also involved in the ice-binding mechanism by hydrogen bonding, as shown in Table 2. This observation concurs with the findings of Hudait and the team, which confirmed that hydrophobic amino acid residues are also crucial in ice-binding, similar to hydrophilic residues (Hudait et al., 2019).

The results of the secondary structure of the selected antifreeze peptides are summarized in Table 3. Among the 8 peptides, only EAAEHLVQEYKDHRL had an alpha-helical structure, while the rest appeared as strands and coiled. Some well-known and documented AFPs have been reported to have a helical structure contributing to their antifreeze activity (Graether et al., 2000; Shah et al., 2012). In their study, Yang and team showed that the high cryoprotective activity of the antifreeze peptide EG-10, EGPRAGGAPG, from *Takifugu Obscurus* skin was related to its alpha-helical structure (Yang et al., 2022). However, based on these properties alone, we cannot solely suggest which specific peptide(s) give shrimp heads their antifreeze properties.

The molecular docking study clearly shows the binding site of the peptides (amino acid residues) involved in ice-binding and the binding interactions. However, antifreeze peptides bind to specific planes on the ice crystal, including prism, pyramidal, and basal faces (Olijve et al., 2016). Molecular simulations of the identified antifreeze peptides with ice/water surfaces can be carried out to gain further insights into the planes involved.
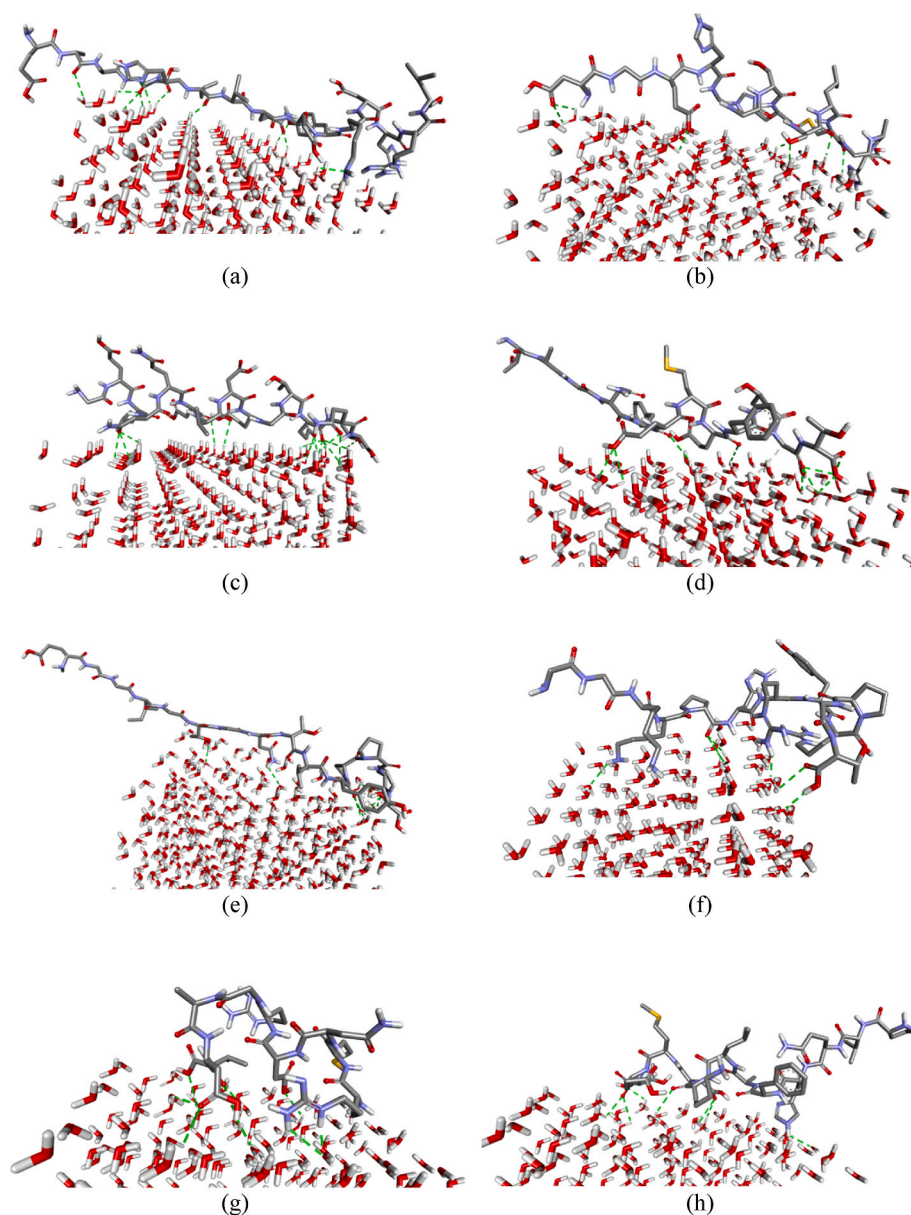
Fig. 6. Molecular docking ice-antifreeze peptide showing ice binding of EAAEHLVQEYKDHRL (a), DGEHGGSHSLCGAH (b), GELNQDVDEGTEQT (c), TAGNFE-MEFTGT (d), EGGIGTGNTVYPPLS (e), GGKKPHRYRPGT (f), IMNDRGADV (g), PVQHFALKDMET (h). Green dashed lines represent hydrogen bonding interaction. (For interpretation of the references to colour in this figure legend, the reader is referred to the Web version of this article.)

Table 2
The binding energy of Ice/water-peptide complexes and ice-binding sites of the peptides.

Peptide Sequence	Binding energy (kCal/mol)	Amino acid residues involved in ice-binding
EAAEHLVQEYKDHRL	−10.2	Ala (2), Glu (4) His (5), Leu (6), Tyr (10), Lys (11)
DGEHGGSHSLCGAH	−7.8	Asp (1), Glu (3), Ser (9), Cys (11)
GELNQDVDEGTEQT	−8.0	Gly (1), Asp (6), Glu (12), Val (7), Gln (13), Thr (14),
TAGNFEMEFTGT	−7.5	Phe (5), Glu (6), Glu (8), Gly (11), Thr (12)
EGGIGTGNTVYPPLS	−7.5	Thr (6), Asn (8), Tyr (11), leu (14)
GGKKPHRYRPGT	−7.3	Lys (4), Pro (5), Arg (7), Thr (12)
IMNDRGADV	−7.4	Ile (1), Asp (4), Asp (8), Val (9)
PVQHFALKDMET	−7.1	His (4), Asp (9), Gln (11), Thr (12)

Table 3
The percentage prediction of secondary structure of selected antifreeze peptides.

Sequence	Alpha helix (Hh)	β-sheet	Random coil (C)	Extended strand
EAAEHLVQEYKDHRL	86.7	–	13.3	–
DGEHGGSHSLCGAH	–	–	64.3	35.7
GELNQDVDEGTEQT	–	–	64.3	35.7
TAGNFEMEFTGT	–	–	58.3	41.7
EGGIGTGNTVYPPLS	–	–	73.3	26.7
GGKKPHRYRPGT	–	–	100	–
IMNDRGADV	–	–	100	–
PVQHFALKDMET	–	–	66.7	33.3

4. Conclusion

Shrimp head autolysate showed an antifreeze effect on peeled shrimps during five F-T cycles, especially at 1.0 and 3.0%-SHA concentrations. Separation by ultrafiltration and ion-exchange chromatography increased the initial TH of shrimp head autolysate (1.82 °C) by 0.02 °C. Molecular docking results show the amino acid residues in shrimp head antifreeze peptides that enabled the AFPs to interact with ice and limit its growth. In summary, antifreeze peptides from shrimp head autolysate have potential applications in the food industry as safe additives in frozen foods to delay the growth of ice crystals during frozen storage. Molecular simulation studies can yield more detailed and valuable insights into the specific ice planes to which these antifreeze peptides bind. Furthermore, the identified antifreeze peptides can be individually synthesized and thoroughly studied to understand their ice-binding mechanisms better.

CRediT authorship contribution statement

Julieth Joram Majura: Writing – original draft, Methodology, Investigation, Data curation, Conceptualization. **Xiujuan Chen:** Methodology, Formal analysis. **Zhongqin Chen:** Supervision, Conceptualization. **Mingtang Tan:** Software, Resources. **Guoping Zhu:** Resources. **Jialong Gao:** Writing – review & editing, Conceptualization. **Haisheng Lin:** Supervision, Resources. **Wenhong Cao:** Writing – review & editing, Supervision, Project administration, Funding acquisition.

Data availability statement

Data supporting the findings of this study are available upon reasonable request from the corresponding author.

Declaration of competing interest

The authors declare that they have no known competing financial interests or personal relationships that could have appeared to influence the work reported in this paper.

Appendix A. Supplementary data

Supplementary data to this article can be found online at https://doi.org/10.1016/j.crfs.2024.100886.

Data availability

Data will be made available on request.

References

Abuzar, Sharif, H.R., Sharif, M.K., Arshad, R., Rehman, A., Ashraf, W., Karim, A., Awan, K.A., Raza, H., Khalid, W., 2023. Potential industrial and nutritional applications of shrimp by-products: a review. Int. J. Food Prop. 26, 3407–3432. https://doi.org/10.1080/10942912.2023.2283378.

Baardsnes, J., Jelokhani-Niaraki, M., Kondejewski, L.H., Kuiper, M.J., Kay, C.M., Hodges, R.S., Davies, P.L., 2001. Antifreeze protein from shorthorn sculpin: identification of the ice-binding surface. Protein Sci. 10, 2566–2576. https://doi.org/10.1110/ps.ps.26501.

Baskaran, A., Kaari, M., Venugopal, G., Manikkam, R., Joseph, J., Bhaskar, P.V., 2021. Anti freeze proteins (Afp): properties, sources and applications–A review. Int. J. Biol. Macromol. 189, 292–305. https://doi.org/10.1016/j.ijbiomac.2021.08.105.

Cahú, T.B., Santos, S.D., Mendes, A., Córdula, C.R., Chavante, S.F., Carvalho Jr., L.B., Nader, H.B., Bezerra, R.S., 2012. Recovery of protein, chitin, carotenoids and

glycosaminoglycans from Pacific white shrimp (*Litopenaeus vannamei*) processing waste. Process Biochem. 47, 570–577. https://doi.org/10.1016/j.procbio.2011.12.012.

Cao, L., Majura, J.J., Liu, L., Cao, W., Chen, Z., Zhu, G., Gao, J., Zheng, H., Lin, H., 2023. The cryoprotective activity of tilapia skin collagen hydrolysate and the structure elucidation of its antifreeze peptide. Lebensm. Wiss. Technol. 179, 114670. https://doi.org/10.1016/j.lwt.2023.114670.

Chen, J., Ying, X., Deng, S., Li, W., Peng, L., Ma, L., 2022. Trehalose and alginate oligosaccharides enhance the stability of myofibrillar proteins in shrimp (*Litopenaeus vannamei*) muscle during frozen storage. J. Food Process. Preserv. 46, e16469. https://doi.org/10.1111/jfpp.16469.

Combet, C., Blanchet, C., Geourjon, C., Deleage, G., 2000. NPS@: network protein sequence analysis. Trends Biochem. Sci. 25, 147–150. https://doi.org/10.1016/S0968-0004(99)01540-6.

Dang, M., Wang, R., Jia, Y., Du, J., Wang, P., Xu, Y., Li, C., 2022. The antifreeze and cryoprotective activities of a novel antifreeze peptide from Ctenopharyngodon idella scales. Foods 11. https://doi.org/10.3390/foods11131830.

Dara, P.K., Geetha, A., Mohanty, U., Raghavankutty, M., Mathew, S., Chandragiri Nagarajarao, R., Rangasamy, A., 2021. Extraction and characterization of myofibrillar proteins from different meat sources: a comparative study. Journal of Bioresources and Bioproducts 6, 367–378. https://doi.org/10.1016/j.jobab.2021.04.004.

Dawson, P., Al-Jeddawi, W., Remington, N., 2018. Effect of freezing on the shelf life of salmon. Int J Food Sci 2018, 1–12. https://doi.org/10.1155/2018/1686121.

Du, X., Li, H., Dong, C., Ren, Y., Pan, N., Kong, B., Liu, H., Xia, X., 2021. Effect of ice structuring protein on the microstructure and myofibrillar protein structure of mirror carp (*Cyprinus carpio L.*) induced by freeze-thaw processes. Lebensm. Wiss. Technol. 139, 110570. https://doi.org/10.1016/j.lwt.2020.110570.

Forli, S., Huey, R., Pique, M.E., Sanner, M.F., Goodsell, D.S., Olson, A.J., 2016. Computational protein–ligand docking and virtual drug screening with the AutoDock suite. Nat. Protoc. 11, 905–919. https://doi.org/10.1038/nprot.2016.051.

Fu, W., Wang, P., Chen, Y., Lin, J., Zheng, B., Zeng, H., Zhang, Y., 2019. Preparation, primary structure and antifreeze activity of antifreeze peptides from *Scomberomorus niphonius* skin. Lebensm. Wiss. Technol. 101, 670–677. https://doi.org/10.1016/j.lwt.2018.11.067.

Gandini, E., Sironi, M., Pieraccini, S., 2020. Modelling of short synthetic antifreeze peptides: insights into ice-pinning mechanism. J. Mol. Graph. Model. 100, 107680. https://doi.org/10.1016/j.jmgm.2020.107680.

Graether, S.P., Kuiper, M.J., Gagné, S.M., Walker, V.K., Jia, Z., Sykes, B.D., Davies, P.L., 2000. β-Helix structure and ice-binding properties of a hyperactive antifreeze protein from an insect. Nature 406, 325–328. https://doi.org/10.1038/35018610.

Graham, L.A., Davies, P.L., 2005. Glycine-rich antifreeze proteins from snow fleas. Science 310, 461. https://doi.org/10.1126/science.1115145, 1979.

Harcum, S., 2008. Purification of protein solutions. In: Biologically Inspired Textiles. Elsevier, pp. 26–43. https://doi.org/10.1533/9781845695088.1.26.

Hudait, A., Qiu, Y., Odendahl, N., Molinero, V., 2019. Hydrogen-bonding and hydrophobic groups contribute equally to the binding of hyperactive antifreeze and ice-nucleating proteins to ice. J. Am. Chem. Soc. 141, 7887–7898. https://doi.org/10.1021/jacs.9b02248.

Jiang, W., Yang, F., Chen, X., Cai, X., Wu, J., Du, M., Huang, J., Wang, S., 2022. Molecular simulation-based research on antifreeze peptides: advances and perspectives. Journal of Future Foods 2, 203–212. https://doi.org/10.1016/j.jfutfo.2022.06.002.

Jommark, N., Runglerdkriangkrai, J., Konno, K., Ratana-arporn, P., 2018. Effect of cryoprotectants on suppression of protein structure deterioration induced by freeze-thaw cycle in Pacific white shrimp. J. Aquat. Food Prod. Technol. 27, 91–106. https://doi.org/10.1080/10498850.2017.1404532.

Knight, C.A., Driggers, E., DeVries, A.L., 1993. Adsorption to ice of fish antifreeze glycopeptides 7 and 8. Biophys. J. 64, 252–259. https://doi.org/10.1016/S0006-3495(93)81361-4.

Krichen, F., Sila, A., Caron, J., Kobbi, S., Nedjar, N., Miled, N., Blecker, C., Besbes, S., Bougatef, A., 2018. Identification and molecular docking of novel ACE inhibitory peptides from protein hydrolysates of shrimp waste. Eng. Life Sci. 18, 682–691. https://doi.org/10.1002/elsc.201800045.

Lee, H., 2019. Effects of hydrophobic and hydrogen-bond interactions on the binding affinity of antifreeze proteins to specific ice planes. J. Mol. Graph. Model. 87, 48–55. https://doi.org/10.1016/j.jmgm.2018.11.006.

Lee, J., Fong, Q., Park, J.W., 2016. Effect of pre-freezing treatments on the quality of Alaska pollock fillets subjected to freezing/thawing. Food Biosci. 16, 50–55. https://doi.org/10.1016/j.fbio.2016.09.00.

Lorentzen, G., Hustad, A., Lian, F., Grip, A.E., Schrøter, E., Medeiros, T., Siikavuopio, S.I., 2020. Effect of freezing methods, frozen storage time, and thawing methods on the quality of mildly cooked snow crab (*Chionoecetes opilio*) clusters. Lebensm. Wiss. Technol. 123, 109103. https://doi.org/10.1016/j.lwt.2020.10910.

Majura, J.J., Han, M., Ouyang, J., Chen, X., Chen, Z., Tan, M., Gao, J., Lin, H., Zheng, H., Cao, W., 2023. The antifreeze activity and physicochemical properties of *Litopenaeus vannamei* head autolysate. Int. J. Food Sci. Technol. 58, 6131–6142. https://doi.org/10.1111/ijfs.16724.

Masson, P., Lushchekina, S., 2022. Conformational stability and denaturation processes of proteins investigated by electrophoresis under extreme conditions. Molecules 27, 6861. https://doi.org/10.3390/molecules27206861.

Nikoo, M., Benjakul, S., Gavlighi, H.A., Xu, X., Regenstein, J.M., 2019. Hydrolysates from rainbow trout (*Oncorhynchus mykiss*) processing by-products: properties when added to fish mince with different freeze-thaw cycles. Food Biosci. 30, 100418. https://doi.org/10.1016/j.fbio.2019.100418.

Nikoo, M., Xu, X., Regenstein, J.M., Noori, F., 2021. Autolysis of Pacific white shrimp (*Litopenaeus vannamei*) processing by-products: enzymatic activities, lipid and protein oxidation, and antioxidant activity of hydrolysates. Food Biosci. 39, 100844. https://doi.org/10.1016/j.fbio.2020.100844.

Olijve, L.L.C., Meister, K., DeVries, A.L., Duman, J.G., Guo, S., Bakker, H.J., Voets, I.K., 2016. Blocking rapid ice crystal growth through nonbasal plane adsorption of antifreeze proteins. Proc. Natl. Acad. Sci. USA 113, 3740–3745. https://doi.org/10.1073/pnas.1524109113.

Ortiz, J.I.L., Quiroga, E., Narambuena, C.F., Riccardo, J.L., Ramirez-Pastor, A.J., 2021. Thermal hysteresis activity of antifreeze proteins: a model based on fractional statistics theory of adsorption. Phys. Stat. Mech. Appl. 575, 126046. https://doi.org/10.1016/j.physa.2021.126046.

Pratiwi, R., Malik, A.A., Schaduangrat, N., Prachayasittikul, V., Wikberg, J.E.S., Nantasenamat, C., Shoombuatong, W., 2017. CryoProtect: a web server for classifying antifreeze proteins from nonantifreeze proteins. J. Chem. 2017, 1–15. https://doi.org/10.1155/2017/9861752.

Ramirez-Guerra, H.E., Garcia-Sifuentes, C.O., Pacheco-Aguilar, R., Ramirez-Suarez, J.C., Lugo-Sánchez, M.E., Scheuren-Acevedo, S.M., 2012. The influence of ante-mortem hypoxia on the physicochemical stability of myofibrillar proteins in the muscle tissue of white shrimp (*Litopenaeus vannamei*) exposed to multiple freeze–thaw cycles. Eur. Food Res. Technol. 235, 37–45. https://doi.org/10.1007/s00217-012-1702-2.

Shah, S.H.H., Kar, R.K., Asmawi, A.A., Rahman, M.B.A., Murad, A.M.A., Mahadi, N.M., Basri, M., Rahman, R.N.Z.A., Salleh, A.B., Chatterjee, S., 2012. Solution structures, dynamics, and ice growth inhibitory activity of peptide fragments derived from an antarctic yeast protein. PLoS One 7, e49788. https://doi.org/10.1371/journal.pone.0049788.

Shi, Y., Wang, H., Zheng, Y., Qiu, Z., Wang, X., 2022. Effects of ultrasound-assisted vacuum impregnation antifreeze protein on the water-holding capacity and texture properties of the yesso scallop adductor muscle during freeze–thaw cycles. Foods 11, 320. https://doi.org/10.3390/foods11030320.

Sun, L., Zhu, Z., Sun, D.-W., 2023. Regulating ice formation for enhancing frozen food quality: materials, mechanisms and challenges. Trends Food Sci. Technol. 139, 104116–104405. https://doi.org/10.1016/j.tifs.2023.07.013.

Tyshenko, M.G., Doucet, D., Davies, P.L., Walker, V.K., 1997. The antifreeze potential of the spruce budworm thermal hysteresis protein. Nat. Biotechnol. 15, 887–890. https://doi.org/10.1038/nbt0997-887.

Walayat, N., Wang, X., Nawaz, A., Zhang, Z., Abdullah, Khalifa, I., Saleem, M.H., Mushtaq, B.S., Pateiro, M., Lorenzo, J.M., 2021. Ovalbumin and kappa-carrageenan mixture suppresses the oxidative and structural changes in the myofibrillar proteins of grass carp (*Ctenopharyngodon idella*) during frozen storage. Antioxidants 10, 1186. https://doi.org/10.3390/antiox10081186.

Wan, W., Feng, J., Wang, H., Du, X., Wang, B., Yu, G., Xia, X., 2023. Influence of repeated freeze-thaw treatments on the oxidation and degradation of muscle proteins from mirror carp (*Cyprinus carpio L.*), based on myofibrillar protein structural changes. Int. J. Biol. Macromol. 226, 454–462. https://doi.org/10.1016/j.ijbiomac.2022.12.082.

Wang, J., Xu, Z., Jiang, L., Zhang, Y., Sui, X., 2023. Further evaluation on structural and antioxidant capacities of soy protein isolate under multiple freeze–thaw cycles. Food Chem. X 17, 100574. https://doi.org/10.1016/j.fochx.2023.100574.

Yan, B., Bai, W., Tao, Y., Ye, W., Zhang, W., Zhang, N., Huang, J., Chen, W., Fan, D., 2023. Physicochemical changes and comparative proteomics analysis of hairtail (*Trichiurus lepturus*) fish muscles during frozen storage. Food Biosci. 55, 103021. https://doi.org/10.1016/j.fbio.2023.103021.

Yang, F., Jiang, W., Chen, Xu, Chen, Xuan, Wu, J., Huang, J., Cai, X., Wang, S., 2022. Identification of novel antifreeze peptides from *Takifugu obscurus* skin and molecular mechanism in inhibiting ice crystal growth. J. Agric. Food Chem. 70, 14148–14156. https://doi.org/10.1021/acs.jafc.2c04393.

Zhang, Y., Kim, Y.H.B., Puolanne, E., Ertbjerg, P., 2022. Role of freezing-induced myofibrillar protein denaturation in the generation of thaw loss: a review. Meat Sci. 190, 108841. https://doi.org/10.1016/j.meatsci.2022.108841.

Zhu, K., Zheng, Z., Dai, Z., 2022. Identification of antifreeze peptides in shrimp byproducts autolysate using peptidomics and bioinformatics. Food Chem. 383, 132568. https://doi.org/10.1016/j.foodchem.2022.132568.